

# UC Santa Barbara

## UC Santa Barbara Previously Published Works

**Title**

Synthesis of a terminal Ce(iv) oxo complex by photolysis of a Ce(iii) nitrate complex.

**Permalink**

<https://escholarship.org/uc/item/8274b60r>

**Journal**

Chemical science, 8(11)

**ISSN**

2041-6520

**Authors**

Assefa, Mikiyas K  
Wu, Guang  
Hayton, Trevor W

**Publication Date**

2017-11-01

**DOI**

10.1039/c7sc03715e

Peer reviewed

Cite this: *Chem. Sci.*, 2017, **8**, 7873

# Synthesis of a terminal Ce(IV) oxo complex by photolysis of a Ce(III) nitrate complex†

Mikiyas K. Assefa,  Guang Wu and Trevor W. Hayton \*

Reaction of  $[\text{Ce}(\text{NR}_2)_3]$  ( $\text{R} = \text{SiMe}_3$ ) with  $\text{LiNO}_3$  in THF, in the presence of 2,2,2-cryptand, results in the formation of the Ce(III) "ate" complex,  $[\text{Li}(2,2,2\text{-cryptand})][\text{Ce}(\kappa^2\text{-O}_2\text{NO})(\text{NR}_2)_3]$  (**1**) in 38% yield. Photolysis of **1** at 380 nm affords  $[\text{Li}(2,2,2\text{-cryptand})][\text{Ce}(\text{O})(\text{NR}_2)_3]$  (**2**), in 33% isolated yield after reaction work-up. Complex **2** is the first reported example of a Ce(IV) oxo complex where the oxo ligand is not supported by hydrogen bonding or alkali metal coordination. Also formed during photolysis are  $[\text{Li}(2,2,2\text{-cryptand})]_2[(\mu_3\text{-O})(\text{Ce}(\mu\text{-O})(\text{NR}_2)_2)_3]$  (**3**) and  $[\text{Li}(2,2,2\text{-cryptand})][\text{Ce}(\text{OSiMe}_3)(\text{NR}_2)_3]$  (**4**). Their identities were confirmed by X-ray crystallography. Complex **4** can also be prepared *via* reaction of  $[\text{Ce}(\text{NR}_2)_3]$  with  $\text{LiOSiMe}_3$  in THF, in the presence of 2,2,2-cryptand. When synthesized in this fashion, **4** can be isolated in 47% yield. To rationalize the presence of **2**, **3**, and **4** in the reaction mixture, we propose that photolysis of **1** first generates **2** and  $\text{NO}_2$ , *via* homolytic cleavage of the N–O bond in its nitrate co-ligand. Complex **2** then undergoes decomposition *via* two separate routes: (1) ligand scrambling and oligomerization to form **3**; and, (2) abstraction of a trimethylsilyl cation to form a transient Ce(IV) silyloxide,  $[\text{Ce}^{\text{IV}}(\text{OSiMe}_3)(\text{NR}_2)_3]$ , followed by  $1\text{e}^-$  reduction to form **4**. Alternatively, complex **4** could form directly *via*  $\text{-SiMe}_3$  abstraction by **2**.

Received 24th August 2017

Accepted 27th September 2017

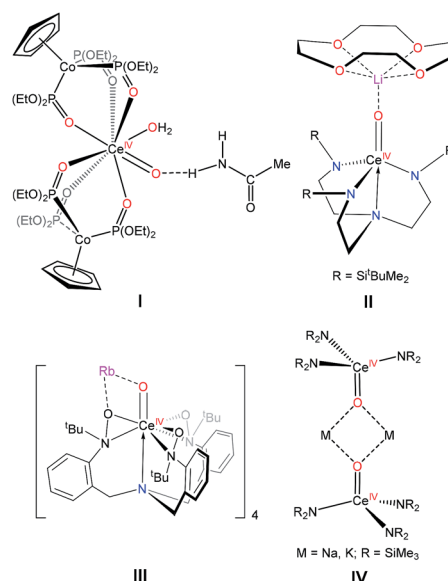
DOI: 10.1039/c7sc03715e

rsc.li/chemical-science

## Introduction

The past five years has seen significant progress made toward the synthesis of lanthanide complexes containing metal–ligand multiple bonds,<sup>1–6</sup> including those featuring  $\text{Ln}=\text{N}$  and  $\text{Ln}=\text{C}$  interactions. For example, Anwander and co-workers recently described the synthesis of the first terminal lanthanide imido complex,  $[(\text{Tp}^{\text{tBu,Me}})\text{Lu}=\text{N}(3,5\text{-(CF}_3)_2\text{C}_6\text{H}_3)(\text{DMAP})]$ , *via* Lewis base-induced methane elimination.<sup>2</sup> Similarly, Schelter and co-workers reported the synthesis of a series of Ce(IV) imido complexes,  $[\text{ML}_n][\text{Ce}=\text{N}(3,5\text{-(CF}_3)_2\text{C}_6\text{H}_3)(\text{TriNOx})]$  ( $\text{TriNOx} = \text{N}(\text{o-CH}_2\text{C}_6\text{H}_4\text{N}^{\text{tBu}}\text{O})_3$ ;  $\text{ML}_n = \text{Li}(\text{THF})(\text{Et}_2\text{O})$ ,  $\text{Li}(\text{TMEDA})$ ,  $\text{K}(\text{DME})_2$ ,  $\text{Rb}(\text{DME})_2$ ,  $\text{Cs}(\text{DME})_2$ ).<sup>5</sup> Significant progress has also been made toward the synthesis of cerium(IV) oxo complexes.<sup>7</sup> For example, Leung and co-workers recently reported the synthesis of a Ce(IV) oxo complex ligated by the tripodal Kläui ligand,  $[(\text{LOEt})_2\text{Ce}(\text{O})(\text{H}_2\text{O})]\cdot\text{MeC}(\text{O})\text{NH}_2$  (**I**,  $\text{LOEt} = \text{CpCo}\{\text{P}(\text{O})(\text{OEt})_2\}_3$ , Scheme 1).<sup>3</sup> Additionally, our group reported the synthesis of the cerium(IV) oxo complex,  $[\text{Li}(12\text{-crown-4})][(\text{NN}'_3)\text{Ce}(\text{O})]$  (**II**,  $\text{NN}'_3 = \text{N}(\text{CH}_2\text{CH}_2\text{NR})_3$ ,  $\text{R} = \text{Si}^{\text{tBu}}\text{Me}_2$ ), which was synthesized by thermal decomposition of a Ce(III) nitrate precursor  $[\text{Li}(12\text{-crown-4})][(\text{NN}'_3)\text{Ce}(\kappa^2\text{-O}_2\text{NO})]$ .<sup>8</sup> More recently,

Schelter and co-workers reported the synthesis of a Ce(IV) oxo supported by the tripodal  $\text{TriNOx}$  ligand,  $[(\text{TriNOx})\{\text{Ce}(\text{O})\}\text{Rb}]_4$  (**III**).<sup>5</sup> Also of note is  $[\text{M}]_2[\text{Ce}(\mu\text{-O})(\text{NR}_2)_3]_2$  (**IV**,  $\text{M} = \text{Na}, \text{K}$ ;  $\text{R} = \text{SiMe}_3$ ), reported by Lappert and co-workers in 2010.<sup>9</sup> These two complexes, which pre-date the other examples mentioned here, were isolated in low yield (*ca.* 20%) upon reaction of



Scheme 1 Selected complexes bearing lanthanide–oxygen multiple bonds.

Department of Chemistry and Biochemistry, University of California Santa Barbara, Santa Barbara, CA 93106, USA. E-mail: hayton@chem.ucsb.edu

† Electronic supplementary information (ESI) available: Further experimental details, figures, spectral, electrochemical, and crystallographic data for **1–4**. CCDC 1569781–1569784. For ESI and crystallographic data in CIF or other electronic format see DOI: 10.1039/c7sc03715e



$\text{Ce}(\text{NR}_2)_3$  with  $\text{MNR}_2$ , in the presence of  $\text{O}_2$ ,<sup>9</sup> but they were not completely characterized.

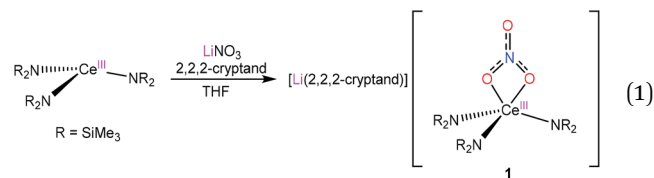
Interestingly, every cerium oxo complex isolated thus far has utilized an external non-covalent interaction to instil stability to this highly reactive functional group. For example, the  $\text{Ce}=\text{O}$  bond in **1** is stabilized by hydrogen bonding to an acetamide solvent molecule.<sup>3</sup> Similarly, the oxo ligands in **II** and **III** are stabilized by their interactions with a capping alkali metal counterion.<sup>5,8</sup> The prevalence of these non-covalent interactions can be rationalized by the poor overlap of the metal f and d orbitals with oxygen 2p orbitals, which results in weak  $\pi$  bonds within the  $\text{Ce}=\text{O}$  fragment, concomitant with considerable oxo nucleophilicity.<sup>4,9–11</sup> Indeed, controlling this nucleophilic character has been one of the key challenges to synthesizing a terminal lanthanide oxo complex.<sup>3</sup>

The unique redox chemistry of the lanthanides also poses a barrier for the synthesis of lanthanide oxo complexes. In particular, cerium redox chemistry is dominated by the  $\text{Ce}(\text{III}/\text{IV})$  redox couple, and thus formation of a  $\text{Ce}(\text{IV})$  oxo complex from a  $\text{Ce}(\text{III})$  precursor essentially mandates a  $1e^-$  O-atom transfer process. However, traditional O-atom transfer reagents, such as  $\text{N}_2\text{O}$ , pyridine-N-oxide, and peroxyacids, are  $2e^-$  oxidants.<sup>12</sup> In our recent synthesis of  $[\text{Li}(\text{12-crown-4})][(\text{NN}'_3)\text{Ce}(\text{O})]$ , the oxo ligand was formed *via* reduction of a nitrate ligand, in a formal  $1e^-$  O-atom transfer process. Several other examples demonstrating the use of nitrate as a  $1e^-$  O-atom source have emerged in recent years,<sup>13–16</sup> suggesting that  $[\text{NO}_3]^-$  could be a valuable reagent for the generation of f-element oxo complexes. This mode of reactivity can also be promoted with light. For example, Berry and co-workers demonstrated that photolysis of  $\text{Ru}_2(\text{chp})_4(\text{NO}_3)$  ( $\text{chp}$  = 6-chloro-2-hydroxypyridinate) generated a metal oxo with concomitant release of  $\text{NO}_2$ .<sup>13</sup> Similarly, Suslick and co-workers reported that photolysis of  $\text{Mn}(\text{TPP})(\text{NO}_3)$  also resulted in metal oxo generation and release of  $\text{NO}_2$ .<sup>15</sup> However, it should be noted that in both of these examples the resulting metal oxo was unstable and not isolated.

Drawing on these results, we sought to further develop the use of  $[\text{NO}_3]^-$  as an O-atom source for the synthesis of f-element oxo complexes. Herein, we describe the photochemical cleavage of nitrate in a  $\text{Ce}(\text{III})$  “ate” precursor to generate the first terminal  $\text{Ce}(\text{IV})$  oxo complex.

## Results and discussion

Reaction of  $[\text{Ce}(\text{NR}_2)_3]$  ( $\text{R} = \text{SiMe}_3$ ) with  $\text{LiNO}_3$  in THF, in the presence of 2,2,2-cryptand, results in the formation of the  $\text{Ce}(\text{III})$  “ate” complex,  $[\text{Li}(2,2,2\text{-cryptand})][\text{Ce}(\kappa^2\text{-O}_2\text{NO})(\text{NR}_2)_3]$  (**1**), which can be isolated as a yellow crystalline solid in 38% yield after work-up (eqn (1)). The  $^1\text{H}$  NMR spectrum of **1** in  $\text{py-d}_5$  displays a broad singlet at  $-1.32$  ppm, assignable to the  $\text{SiMe}_3$  environment, and three resonances at 2.48, 3.45 and 3.51 ppm, assignable to the cryptand moiety. The chemical shift of the methyl resonance, along with its broad appearance, support the presence of a paramagnetic  $\text{Ce}(\text{III})$  centre in this complex. The  $^7\text{Li}\{^1\text{H}\}$  NMR spectrum reveals a broad resonance at  $-1.08$  ppm, indicative of a single lithium environment.



The solid-state molecular structure of **1** (Fig. 1) reveals a  $\kappa^2$  coordination mode of the nitrate ligand, similar to that observed for the cerium(III) nitrate TREN complex,  $[\text{Li}(\text{12-crown-4})][(\text{NN}'_3)\text{Ce}(\text{NO}_3)]$ .<sup>8</sup> However, the  $\text{Ce}-\text{O}$  distances in **1** (2.653(2) and 2.562(2) Å) are shorter than those observed for  $[\text{Li}(\text{12-crown-4})][(\text{NN}'_3)\text{Ce}(\text{NO}_3)]$  (2.724(6) and 2.745(6) Å), likely because of the bulkier TREN ligand in the latter and the absence of Li–O interactions in the former. In addition, the  $\text{Ce}-\text{N}$  distances in **1** (2.367(2)–2.398(2) Å) are consistent with the  $\text{Ce}-\text{N}$  distances reported for other  $\text{Ce}(\text{III})$  amido complexes.<sup>17–20</sup> For comparison, the  $\text{Ce}-\text{N}$  distances in  $\text{Ce}(\text{TMP})_3(\text{THF})$  ( $\text{TMP}$  = 2,2,6,6-tetramethylpiperidinato) range from 2.346(2)–2.374(2) Å, while the distances in  $[\text{Li}(\text{THF})][\text{Ce}(\text{NCy}_2)_4]$  range from 2.320(2)–2.330(2) Å.<sup>18,19</sup> The lithium counter-ion in **1** is encapsulated by the 2,2,2-cryptand moiety, rendering **1** a separated cation–anion pair. Interestingly, only five of the eight donor atoms in the cryptand moiety are bound to the lithium ion; two nitrogen atoms and one oxygen atom remain uncoordinated. Similar binding modes have been observed in other  $[\text{Li}(2,2,2\text{-cryptand})]^+$  complexes.<sup>21–24</sup>

With complex **1** in hand, we explored its suitability as a  $\text{Ce}(\text{IV})$  oxo precursor. Unlike  $[\text{Li}(\text{12-crown-4})][(\text{NN}'_3)\text{Ce}(\text{NO}_3)]$ , however, which is mostly consumed upon standing at room temperature for 24 h, we discovered that complex **1** is not especially temperature sensitive. A  $\text{py-d}_5$  solution of **1**, which was stored

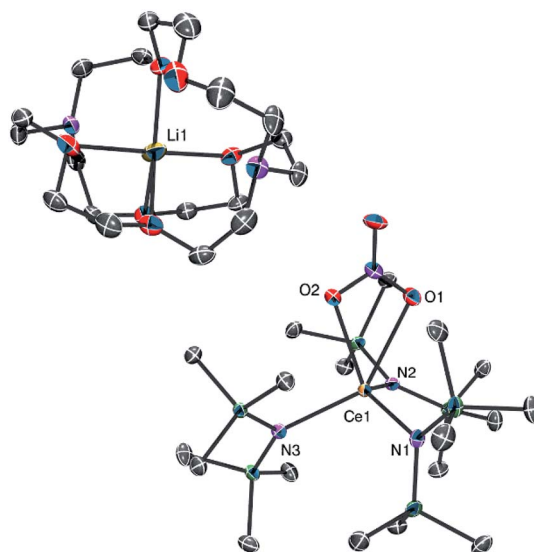


Fig. 1 ORTEP diagram of **1** shown with 50% probability ellipsoids. Hydrogen atoms are omitted for clarity. Selected bond distances (Å) and angles (°):  $\text{Ce1}-\text{O1} = 2.653(2)$ ,  $\text{Ce1}-\text{O2} = 2.562(2)$ ,  $\text{Ce1}-\text{N1} = 2.385(3)$ ,  $\text{Ce1}-\text{N2} = 2.367(2)$ ,  $\text{Ce1}-\text{N3} = 2.398(2)$ ,  $\text{N2}-\text{Ce1}-\text{N1} = 121.01(8)$ ,  $\text{N2}-\text{Ce1}-\text{N3} = 112.82(8)$ ,  $\text{N1}-\text{Ce1}-\text{N3} = 101.96(9)$ .



for 24 h at room temperature in the absence of light, still consisted primarily of complex **1**, as determined by  $^1\text{H}$  NMR spectroscopy. However, we do observe the formation of several new species in this sample, in small amounts, as revealed by resonances at 0.69, 0.20, and  $-0.58$  ppm (see Fig. S10 in the ESI†). These were later identified as belonging to  $[\text{Li}(2,2,2\text{-cryptand})][\text{Ce}(\text{O})(\text{NR}_2)_3]$  (**2**),  $[\text{Li}(2,2,2\text{-cryptand})]_2[(\mu_3\text{-O})\{\text{Ce}(\mu\text{-O})(\text{NR}_2)_2\}_3]$  (**3**), and  $[\text{Li}(2,2,2\text{-cryptand})][\text{Ce}(\text{OSiMe}_3)(\text{NR}_2)_3]$  (**4**), respectively (*vide infra*). These three complexes were present in a relative ratio of 2 : 27 : 1. The relatively high thermal stability of **1** led us to conclude that formation of a terminal Ce(IV) oxo complex through thermal activation of the nitrate co-ligand in **1** was not synthetically viable.

Given the relatively high thermal stability of **1**, we sought an alternative route to reduce its nitrate co-ligand. Schelter and co-workers previously reported that photolysis of  $[\text{Ce}(\text{NR}_2)_3]$  resulted in formation of a relatively long-lived excited state.<sup>25,26</sup> This excited state species is strongly reducing, and can elicit homolytic cleavage of the C–Cl bond in  $\text{PhCH}_2\text{Cl}$ , resulting in formation of  $[\text{Ce}(\text{Cl})(\text{NR}_2)_3]$  and bibenzyl.<sup>25</sup> The UV-vis spectrum of **1** features two absorptions at 380 nm ( $\epsilon = 200 \text{ M}^{-1} \text{ cm}^{-1}$ ) and 336 nm ( $\epsilon = 140 \text{ M}^{-1} \text{ cm}^{-1}$ ) (Fig. S14†), and is similar to that reported for  $[\text{Ce}(\text{NR}_2)_3]$ .<sup>25</sup> We have assigned the former absorption to a metal-based  $4f \rightarrow 5d_{z^2}$  transition and the latter to a  $4f \rightarrow 5d_{xz/yz}$  transition, by analogy with the assignments reported for  $[\text{Ce}(\text{NR}_2)_3]$ . For comparison, these transitions occur at 413 nm and 341 nm, respectively, in  $[\text{Ce}(\text{NR}_2)_3]$ . We attribute the *ca.* 30 nm blue shift observed for the  $4f \rightarrow 5d_{z^2}$  transition in **1** to the presence of the additional nitrate co-ligand, as well as its overall negative charge.

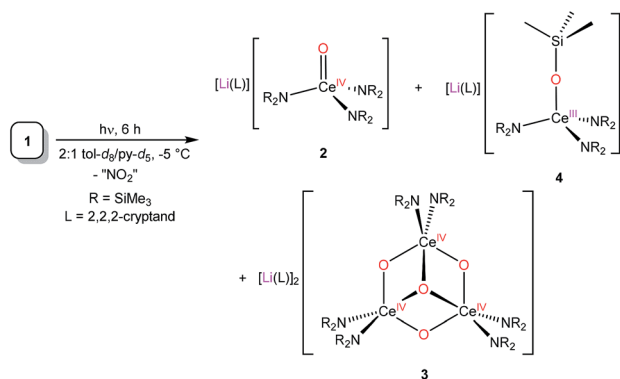
Given the similar optical properties of **1** and  $[\text{Ce}(\text{NR}_2)_3]$ , we hypothesized that photolysis of **1** would induce reduction of the nitrate ligand to afford a Ce(IV) oxo complex. To this end, a 2 : 1 *tol-d*<sub>8</sub>/*py-d*<sub>5</sub> solution of **1**, in an NMR tube equipped with a J-Young valve, was exposed to light from a 380 nm LED lightstrip for 6 h at  $-5^\circ\text{C}$  (Scheme 2). A  $^1\text{H}$  NMR spectrum of this sample revealed an approximately 80% consumption of **1**, as evidenced by the attenuation of its  $\text{SiMe}_3$  resonance at  $-1.18$  ppm. In addition, we observe the appearance of a sharp singlet at 0.80 ppm, as well as the appearance of broad singlets at 0.28,  $-0.21$ , and  $-0.43$  ppm (see Fig. S3 in ESI†). We assigned

the sharp singlet at 0.80 ppm to the terminal Ce(IV) oxo complex  $[\text{Li}(2,2,2\text{-cryptand})][\text{Ce}(\text{O})(\text{NR}_2)_3]$  (**2**), while we have tentatively assigned the resonance at 0.28 ppm to the Ce(IV) oxo cluster  $[\text{Li}(2,2,2\text{-cryptand})]_2[(\mu_3\text{-O})\{\text{Ce}(\mu\text{-O})(\text{NR}_2)_2\}_3]$  (**3**). In addition, the resonances at  $-0.21$  and  $-0.43$  ppm, which integrate to 9 and 54 protons, respectively, are assignable to the Ce(III) siloxide  $[\text{Li}(2,2,2\text{-cryptand})][\text{Ce}(\text{OSiMe}_3)(\text{NR}_2)_3]$  (**4**). After 6 h of photolysis, these three species were present in an approximately 11 : 2.5 : 1 ratio, according to NMR spectroscopy (Fig. S4†). Attempts to photolyse the reaction mixture for longer times, in an attempt to get complete consumption of **1**, lead to decreased yields of **2**. We also found that the use of the 2 : 1 *tol-d*<sub>8</sub>/*py-d*<sub>5</sub> solvent system was critical to maximize the amount of **2** formed in the reaction mixture. If we perform the photolysis in neat *py-d*<sub>5</sub>, the relative amount of **2** decreased substantially; under these conditions complexes **2** and **3** are formed in nearly equal amounts. Moreover, photolyses performed in neat *tol-d*<sub>8</sub> proved impractical because of the low solubility of complex **1** in that solvent. Finally, we observed that photolyses conducted in NMR tubes result in the most efficient consumption of **1**, likely due to their high surface-to-volume ratio.

Work-up of the reaction mixture resulted in the isolation of complex **2** as yellow plates in 33% yield. Its formulation was confirmed by X-ray crystallography (see below). In one instance, we also observed the deposition of small amounts of pale yellow crystals and colorless plates, which were subsequently identified as **3** and **4**, respectively, by X-ray crystallography.

Complex **2** crystallizes in the monoclinic space group  $P2_1/c$  (Fig. 2). In the solid state, **2** displays a terminal Ce=O linkage and a pseudo-tetrahedral geometry about the cerium centre. Its Ce–O bond length (1.840(7) Å) is shorter than those observed for **II** (1.902(2) Å), **III** (1.887(4)–1.902(4) Å), and **IV** (1.908(3) Å),<sup>5,8,9</sup> possibly because of the absence of any alkali metal–oxo interaction in **2**.<sup>5,8</sup> The Ce–O distance in **2** is also shorter than that calculated for  $[\text{K}(18\text{-crown-6})][\text{Ce}(\text{O})(\text{NR}_2)_3]$  (1.904 Å), which also features an alkali metal–oxo interaction.<sup>8</sup> Interestingly, however, the Ce–O distance in **2** is identical to that observed for hydrogen-bond stabilized **I** (1.857(3) Å) by the  $3\sigma$  criterion,<sup>3</sup> suggesting that the hydrogen bonding interaction in **I** does not substantially disrupt the Ce=O bond. Also of note, the Ce–N distances in **2** (2.353(8)–2.397(8) Å) are slightly longer than those reported for other Ce(IV) amides. For example, the Ce–N distances in  $\text{Ce}(\text{NCy}_2)_4$  range from 2.238(5) to 2.247(6) Å, while those of  $[\text{Ce}(\text{X})(\text{NR}_2)_3]$  (X = Cl, Br) are 2.217(3) and 2.219(7) Å, respectively.<sup>19,27,28</sup> This lengthening may be a consequence of the strongly donating nature of the oxo ligand, along with the complex's overall negative charge, which weakens the Ce–N bonds. For further comparison,  $[\text{Li}(12\text{-crown-4})][(\text{NN}'_3)\text{Ce}(\text{O})]$  also features longer than expected Ce–N distances.<sup>8</sup> Finally, the Li-binding mode of the 2,2,2-cryptand moiety in **2** is similar to that observed in **1**. However, in **2**, six of the eight donor atoms in the cryptand moiety are bound to the lithium ion; only one nitrogen atom and one oxygen atom remain uncoordinated.

Complex **2** is soluble in toluene,  $\text{Et}_2\text{O}$ , benzene, and pyridine, but decomposes when exposed to THF, acetonitrile, and dichloromethane (forming  $\text{HN}(\text{SiMe}_3)_2$  as the only identifiable product). Its  $^1\text{H}$  NMR spectrum in *py-d*<sub>5</sub> features a sharp singlet



Scheme 2 Synthesis of complexes **2**, **3**, and **4** via photolysis of **1**.



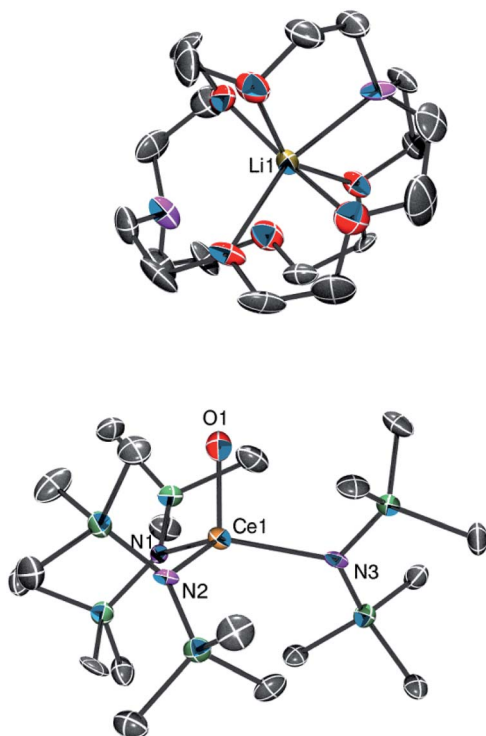


Fig. 2 ORTEP diagram of **2** shown with 50% probability ellipsoids. Hydrogen atoms are omitted for clarity. Selected bond distances (Å) and angles (°): Ce1–O1 = 1.840(7), Ce1–N1 = 2.397(8), Ce1–N2 = 2.353(8), Ce1–N3 = 2.383(8), N2–Ce1–N1 = 116.4(3), N3–Ce1–N1 = 113.4(3), N2–Ce1–N3 = 116.8(3), O1–Ce1–N1 = 103.9(3), O1–Ce1–N2 = 101.7(3), O1–Ce1–N3 = 101.5(3).

at 0.69 ppm integrating to 54 protons, which is assignable to the  $\text{SiMe}_3$  environment, while the resonances at 2.56, 3.52, and 3.59 ppm, each integrating to 12 protons, are assignable to the cryptand moiety. The chemical shift of its  $\text{SiMe}_3$  resonance is nearly identical to that assigned to this complex in the spectrum of the crude reaction mixture (Fig. S4†). The  $^7\text{Li}\{\text{H}\}$  NMR spectrum of **2** features a broad singlet centred at  $-1.00$  ppm. This chemical shift is in the range previously reported for the  $[\text{Li}(2,2,2\text{-cryptand})]^+$  ion.<sup>29,30</sup> We also recorded the Raman spectrum of **2**, but were unable to make a definitive assignment of the  $\text{Ce}=\text{O}$  stretch. Finally, we have found that complex **2** is somewhat thermally sensitive. Upon standing in  $2 : 1$   $\text{tol-}d_8/\text{py-}d_5$  at room temperature for 4 d, complex **2** decomposes to a mixture of **3**, **4**, and  $\text{LiN}(\text{SiMe}_3)_2$  (along with other unidentified products) with about 70% conversion (Fig. S12 and S13†). Under these conditions, complexes **3** and **4** are present in an approximately 3 : 1 ratio. Similar results are observed when **2** is left to stand in neat  $\text{py-}d_5$  (Fig. S11†).

Complex **3** crystallizes in triclinic space group  $P\bar{1}$  (Fig. 3). In the solid state, complex **3** consists of a partial cubane  $\text{Ce}_3\text{O}_4$  core. Each Ce centre is also ligated by two silylamide ligands. Additionally, **3** features two  $[\text{Li}(2,2,2\text{-cryptand})]^+$  counterions, confirming the tetravalent oxidation state of each cerium atom. The Ce–O distances observed for the three  $\mu_2$ -oxo ligands in **3** range from 2.071(7) to 2.133(7) Å, and are comparable to those observed in the structurally related Ce(IV) oxo cluster,  $[(\mu\text{-O})$

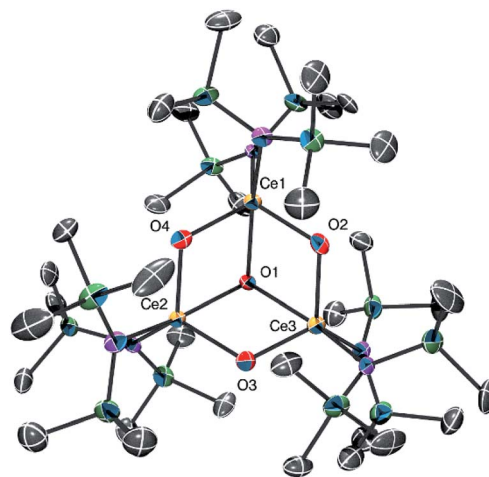


Fig. 3 ORTEP diagram of **3** shown with 50% probability ellipsoids. Hydrogen atoms, diethyl ether solvate and two  $[\text{Li}(2,2,2\text{-cryptand})]^+$  counter-ions are omitted for clarity. Selected bond distances (Å) and angles (°): Ce1–O1 = 2.294(7), Ce1–O2 = 2.078(7), Ce1–O4 = 2.133(7), Ce2–O1 = 2.310(7), Ce2–O3 = 2.109(7), Ce2–O4 = 2.071(7), Ce3–O1 = 2.289(7), Ce3–O2 = 2.130(7), Ce3–O3 = 2.100(7), Ce1–N1 = 2.391(8), Ce1–N2 = 2.366(8), Ce2–N5 = 2.389(8), Ce2–N6 = 2.380(9), Ce3–N3 = 2.386(9), Ce3–N4 = 2.415(9), Ce3–O1–Ce1 = 99.8(3), Ce3–O1–Ce2 = 99.6(3), Ce1–O1–Ce2 = 99.5(3).

$\text{Ce}(\text{NR}_2)_3$ ],<sup>9</sup> reported by Lappert and co-workers. The Ce–O distances observed for the  $\mu_3$ -oxo ligand in **3** are longer, ranging from 2.289(7) to 2.310(7) Å, but are similar to those reported for other known  $[\text{Ce}_3(\mu_3\text{-oxo})]$  clusters.<sup>31,32</sup> We can rule out the presence of a hydroxo ligand in **3** on the basis of our structural data. In particular, the Ce–O distances of  $\mu_2$ - or  $\mu_3$ -hydroxo ligands are anticipated to be substantially longer than the Ce–O distances observed for **2**.<sup>33,34</sup> As was observed for **2**, the Ce–N distances in **3** (2.366(8)–2.415(9) Å) are somewhat longer than those typically reported for Ce(IV) amides.<sup>19,27,28</sup> Unfortunately, we have been unable to isolate pure samples of **3**, and thus have been unable to complete its characterization. As such, the NMR spectroscopic assignments that we report for this complex (see above) should be considered tentative.

Complex **4** crystallizes in the monoclinic space group  $P2_1/n$  and its solid-state molecular structure is shown in Fig. 4. In the solid state, complex **4** consists of a pseudo-tetrahedral Ce(III) anion and a  $[\text{Li}(2,2,2\text{-cryptand})]^+$  cation. Complex **4** features a Ce–O bond length of 2.214(3) Å which is significantly longer than the Ce–O distance found in **2** (1.840(7) Å), further supporting the presence of  $\text{Ce}=\text{O}$  multiple bond character in the latter. However, this distance is similar to the average Ce–O $_{\text{SiPh}_3}$  distance in  $\text{Ce}(\text{OSiPh}_3)_3(\text{THF})_3$  (2.22 Å).<sup>35</sup> The average Ce–N distance in **4** (2.41 Å) is comparable to that observed for **1** (2.38 Å), consistent with its anticipated Ce(III) oxidation state. Finally, the Ce–O–Si bond angle ( $178.9(2)^\circ$ ) is similar to that observed for  $\text{Ce}(\text{OSiPh}_3)_3(\text{THF})_3$  (av.  $174^\circ$ )<sup>35</sup> and  $[(\text{NN}'_3)\text{Ce}(\text{OSiMe}_2\text{tBu})]$  ( $167.2(2)^\circ$ ).<sup>8</sup>

Conveniently, complex **4** can be synthesized independently via reaction of  $[\text{Ce}(\text{NR}_2)_3]$  with  $\text{LiOSiMe}_3$  in THF, in the presence of 2,2,2-cryptand (eqn (2)), permitting its complete





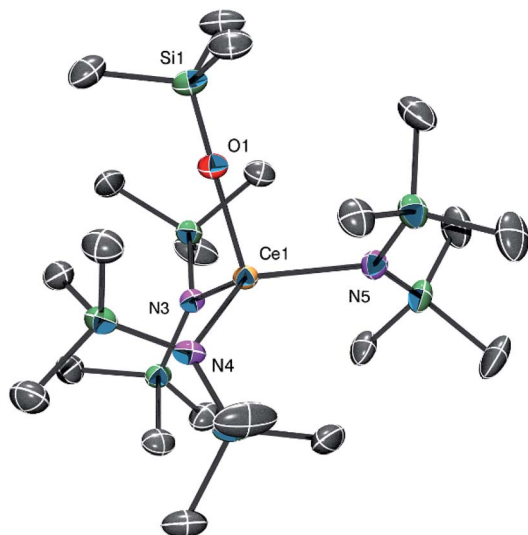
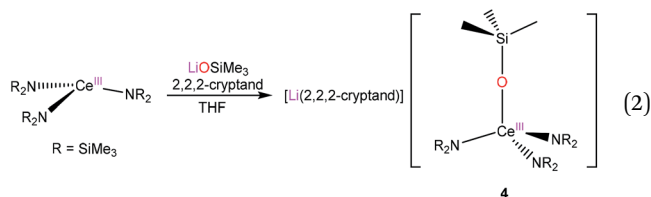


Fig. 4 ORTEP diagram of **4** shown with 50% probability ellipsoids. Hydrogen atoms and [Li(2,2,2-cryptand)] counterion are omitted for clarity. Selected bond distances (Å) and angles (°): Ce1–O1 = 2.214(3), Ce1–N3 = 2.430(4), Ce1–N4 = 2.396(4), Ce1–N5 = 2.413(4), O1–Si1 = 1.607(4), N4–Ce1–N3 = 109.97(13), N4–Ce1–N5 = 117.68(14), N5–Ce1–N3 = 117.42(13), Si1–O1–Ce1 = 178.9(2).

characterization. Synthesized *via* this route, **4** can be isolated as a white solid in 47% yield after work-up.



The  $^1\text{H}$  NMR spectrum of **4** in  $\text{py-d}_5$  features two broad singlets at  $-0.37$  and  $-0.59$  ppm, integrating to 9 and 54 protons, respectively. These resonances are assignable to the  $\text{OSiMe}_3$  and  $\text{N}(\text{SiMe}_3)_2$  methyl environments, respectively. Importantly, these resonances are nearly identical to those assigned to this complex in the spectrum of crude reaction mixture (Fig. S4†). Also observed in the  $^1\text{H}$  NMR spectrum of **4** are resonances at 2.56, 3.52 and 3.60 ppm, each integrating to 12 protons, which are assignable to the cryptand moiety. Finally, its  $^7\text{Li}\{^1\text{H}\}$  NMR spectrum consists of a single resonance at  $-0.97$  ppm.

To rationalize the presence of **2**, **3**, and **4** in the reaction mixture, we propose that photolysis of **1** first generates **2** and  $\text{NO}_2$ , *via* homolytic cleavage of the N–O bond in its nitrate co-ligand. However, **2** is unstable to the reaction conditions and begins to decompose *via* two separate routes: (1) ligand scrambling and oligomerization to form **3**; and, (2) abstraction of a trimethylsilyl cation to form a transient  $\text{Ce}(\text{IV})$  silyloxide,  $[\text{Ce}^{\text{IV}}(\text{OSiMe}_3)(\text{NR}_2)_3]$ , followed by  $1\text{e}^-$  reduction to form **4**. Alternatively, complex **4** could form directly *via*  $\cdot\text{SiMe}_3$  abstraction by **2**. To support these hypotheses, we note that complex **2** is thermally unstable, and slowly decomposes to

form a mixture of **3** and **4** in solution (Fig. S12 and S13†). Additionally, we observe a minor resonance at 0.53 ppm in the  $^1\text{H}$  NMR spectrum of the photolysis reaction mixture (Fig. S4†), which is assignable to  $\text{LiN}(\text{SiMe}_3)_2$ . Its presence is consistent with the proposed conversion of **2** to **3** *via* ligand scrambling and loss of  $\text{LiN}(\text{SiMe}_3)_2$ . Finally, we previously demonstrated that the  $\text{Ce}(\text{IV})$  silyloxide,  $[(\text{NN}')_3\text{Ce}(\text{OSi}^t\text{BuMe}_2)]$ , was formed as a minor by-product during the conversion of  $[\text{Li}(12\text{-crown-4})][(\text{NN}')_3\text{Ce}(\kappa^2\text{-O}_2\text{NO})]$  to the  $\text{Ce}(\text{IV})$  oxo,  $[\text{Li}(12\text{-crown-4})][(\text{NN}')_3\text{Ce}(\text{O})]$ ,<sup>8</sup> presumably *via* a similar adventitious  $[\text{SiR}_3]^+$  abstraction.

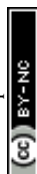
To test the thermodynamic favourability of the proposed  $1\text{e}^-$  reduction to form **4**, we investigated its electrochemistry by cyclic voltammetry. The cyclic voltammogram of **4** in THF reveals a redox feature centred at  $-0.53$  V at  $200\text{ mV s}^{-1}$  (vs.  $\text{Fc}/\text{Fc}^+$ ; see Fig. S23 in ESI†). This feature is marked by a large difference between the potentials of the oxidation and reduction peaks (*i.e.*,  $0.72$  V at  $200\text{ mV s}^{-1}$ ), suggestive of an ECE-type process. While the potential of this feature is comparable to those previously reported for cerium complexes with similar ligand frameworks, including  $[\text{Ce}(\text{F})(\text{NR}_2)_3]$  ( $-0.56$  V),  $[\text{Ce}(\text{Cl})(\text{NR}_2)_3]$  ( $-0.30$  V) and  $[\text{Ce}(\text{Br})(\text{NR}_2)_3]$  ( $-0.31$  V),<sup>36–38</sup> its electrochemical irreversibility suggests that  $[\text{Ce}^{\text{IV}}(\text{OSiMe}_3)(\text{NR}_2)_3]$  is not particularly stable. Therefore, complex **4** may not be formed *via* a straightforward  $1\text{e}^-$  reduction of a  $[\text{Ce}^{\text{IV}}(\text{OSiMe}_3)(\text{NR}_2)_3]$  intermediate. Instead, the cyclic voltammetry data may be evidence for a concerted  $\cdot\text{SiMe}_3$  abstraction by **2** to form **4**. A similar  $\cdot\text{SiMe}_3$  abstraction by the uranyl fragment has been reported by Arnold and co-workers.<sup>39–41</sup>

## Conclusions

In summary, we report the synthesis of the first lanthanide oxo complex where the oxo ligand is not supported by hydrogen bonding or alkali metal coordination, namely,  $[\text{Li}(2,2,2\text{-cryptand})][\text{Ce}(\text{O})(\text{NR}_2)_3]$  (**2**). This complex was generated by photolysis of the  $\text{Ce}(\text{III})$  nitrate precursor  $[\text{Li}(2,2,2\text{-cryptand})][\text{Ce}(\kappa^2\text{-O}_2\text{NO})(\text{NR}_2)_3]$  (**1**), which results in photochemical cleavage of the nitrate co-ligand. Also formed in the photolysis reaction are the  $\text{Ce}(\text{IV})$  oxo cluster,  $[\text{Li}(2,2,2\text{-cryptand})]_2[(\mu_3\text{-O})\{\text{Ce}(\mu\text{-O})(\text{NR}_2)_2\}_3]$  (**3**), and the  $\text{Ce}(\text{III})$  silyloxide complex,  $[\text{Li}(2,2,2\text{-cryptand})][\text{Ce}(\text{OSiMe}_3)(\text{NR}_2)_3]$  (**4**). We believe these two complexes are formed upon thermal (or photochemical) decomposition of **2** after its initial generation in the reaction mixture. Overall, this work further highlights the utility of  $[\text{NO}_3]^-$  as a  $1\text{e}^-$  O-atom source for the generation of lanthanide oxo complexes. Indeed, we have now shown that nitrate reduction to form cerium oxos can proceed *via* both thermal and photochemical routes. Going forward, we will attempt to synthesize a  $\text{Ln}(\text{III})$  oxo complex *via*  $1\text{e}^-$  O-atom transfer from  $[\text{NO}_3]^-$ . This is anticipated to be a greater synthetic challenge because the lower Ln oxidation state results in reduced Ln–O bond covalency.<sup>42</sup>

## Conflicts of interest

There are no conflicts to declare.



## Acknowledgements

We thank the National Science Foundation (CHE 1361654) for financial support of this work. This research made use of the 400 MHz NMR Spectrometer of the Chemistry Department, an NIH SIG (1S10OD012077-01A1).

## Notes and references

- 1 M. Gregson, E. Lu, J. McMaster, W. Lewis, A. J. Blake and S. T. Liddle, *Angew. Chem., Int. Ed.*, 2013, **52**, 13016–13019.
- 2 D. Schädle, M. Meermann-Zimmermann, C. Schädle, C. Maichle-Mössmer and R. Anwender, *Eur. J. Inorg. Chem.*, 2015, **2015**, 1334–1339.
- 3 Y.-M. So, G.-C. Wang, Y. Li, H. H. Y. Sung, I. D. Williams, Z. Lin and W.-H. Leung, *Angew. Chem., Int. Ed.*, 2014, **53**, 1626–1629.
- 4 O. T. Summerscales and J. C. Gordon, *RSC Adv.*, 2013, **3**, 6682–6692.
- 5 L. A. Solola, A. V. Zabula, W. L. Dorfner, B. C. Manor, P. J. Carroll and E. J. Schelter, *J. Am. Chem. Soc.*, 2017, **139**, 2435–2442.
- 6 L. A. Solola, A. V. Zabula, W. L. Dorfner, B. C. Manor, P. J. Carroll and E. J. Schelter, *J. Am. Chem. Soc.*, 2016, **138**, 6928–6931.
- 7 Y.-M. So, Y. Li, K.-C. Au-Yeung, G.-C. Wang, K.-L. Wong, H. H. Y. Sung, P. L. Arnold, I. D. Williams, Z. Lin and W.-H. Leung, *Inorg. Chem.*, 2016, **55**, 10003–10012.
- 8 P. L. Damon, G. Wu, N. Kaltsoyannis and T. W. Hayton, *J. Am. Chem. Soc.*, 2016, **138**, 12743–12746.
- 9 M. P. Coles, P. B. Hitchcock, A. V. Khvostov, M. F. Lappert, Z. Li and A. V. Protchenko, *Dalton Trans.*, 2010, **39**, 6780–6788.
- 10 J. Hong, L. Zhang, X. Yu, M. Li, Z. Zhang, P. Zheng, M. Nishiura, Z. Hou and X. Zhou, *Chem.-Eur. J.*, 2011, **17**, 2130–2137.
- 11 J. Scott, H. Fan, B. F. Wicker, A. R. Fout, M.-H. Baik and D. J. Mindiola, *J. Am. Chem. Soc.*, 2008, **130**, 14438–14439.
- 12 R. H. Holm, *Chem. Rev.*, 1987, **87**, 1401–1449.
- 13 A. R. Corcos, J. S. Pap, T. Yang and J. F. Berry, *J. Am. Chem. Soc.*, 2016, **138**, 10032–10040.
- 14 R. J. Radford, M. D. Lim, R. S. D. Silva and P. C. Ford, *J. Coord. Chem.*, 2010, **63**, 2743–2749.
- 15 K. S. Suslick and R. A. Watson, *Inorg. Chem.*, 1991, **30**, 912–919.
- 16 R. D. Taylor, P. G. Todd, N. D. Chasteen and J. T. Spence, *Inorg. Chem.*, 1979, **18**, 44–48.
- 17 S. D. Daniel, J.-S. M. Lehn, J. D. Korp and D. M. Hoffman, *Polyhedron*, 2006, **25**, 205–210.
- 18 P. B. Hitchcock, Q.-G. Huang, M. F. Lappert and X.-H. Wei, *J. Mater. Chem.*, 2004, **14**, 3266–3273.
- 19 P. B. Hitchcock, M. F. Lappert and A. V. Protchenko, *Chem. Commun.*, 2006, 3546–3548.
- 20 D. Schneider, T. Spallek, C. Maichle-Mössmer, K. W. Tornroos and R. Anwender, *Chem. Commun.*, 2014, **50**, 14763–14766.
- 21 A. N. Chekhlov, *Russ. J. Coord. Chem.*, 2003, **29**, 828–832.
- 22 R. E. A. Dillon, C. L. Stern and D. F. Shriver, *Solid State Ionics*, 2000, **133**, 247–255.
- 23 A. Moores, L. Ricard, P. Le Floch and N. Mézailles, *Organometallics*, 2003, **22**, 1960–1966.
- 24 P. A. Rudd, N. Planas, E. Bill, L. Gagliardi and C. C. Lu, *Eur. J. Inorg. Chem.*, 2013, **2013**, 3898–3906.
- 25 H. Yin, P. J. Carroll, J. M. Anna and E. J. Schelter, *J. Am. Chem. Soc.*, 2015, **137**, 9234–9237.
- 26 H. Yin, P. J. Carroll, B. C. Manor, J. M. Anna and E. J. Schelter, *J. Am. Chem. Soc.*, 2016, **138**, 5984–5993.
- 27 O. Eisenstein, P. B. Hitchcock, A. G. Hulkes, M. F. Lappert and L. Maron, *Chem. Commun.*, 2001, 1560–1561.
- 28 P. B. Hitchcock, A. G. Hulkes and M. F. Lappert, *Inorg. Chem.*, 2004, **43**, 1031–1038.
- 29 E. Pasgreta, R. Puchta, M. Galle, N. van Eikema Hommes, A. Zahl and R. van Eldik, *J. Inclusion Phenom. Macrocyclic Chem.*, 2007, **58**, 81–88.
- 30 R. R. Rhinebarger and A. I. Popov, *Polyhedron*, 1988, **7**, 1341–1347.
- 31 H. C. Aspinall, J. Bacsá, A. C. Jones, J. S. Wrench, K. Black, P. R. Chalker, P. J. King, P. Marshall, M. Werner, H. O. Davies and R. Odedra, *Inorg. Chem.*, 2011, **50**, 11644–11652.
- 32 J. Schläfer, S. Stucky, W. Tyrra and S. Mathur, *Inorg. Chem.*, 2013, **52**, 4002–4010.
- 33 J.-S. M. Lehn and D. M. Hoffman, CCDC 272487: CSD Communication, 2014, DOI: 10.5517/cc94jxv.
- 34 L. Natrajan, J. Pécaut, M. Mazzanti and C. LeBrun, *Inorg. Chem.*, 2005, **44**, 4756–4765.
- 35 P. S. Gradeff, K. Yunlu, T. J. Deming, J. M. Olofson, R. J. Doedens and W. J. Evans, *Inorg. Chem.*, 1990, **29**, 420–424.
- 36 J. R. Robinson, P. J. Carroll, P. J. Walsh and E. J. Schelter, *Angew. Chem., Int. Ed.*, 2012, **51**, 10159–10163.
- 37 U. J. Williams, P. J. Carroll and E. J. Schelter, *Inorg. Chem.*, 2014, **53**, 6338–6345.
- 38 U. J. Williams, J. R. Robinson, A. J. Lewis, P. J. Carroll, P. J. Walsh and E. J. Schelter, *Inorg. Chem.*, 2014, **53**, 27–29.
- 39 P. L. Arnold, D. Patel, C. Wilson and J. B. Love, *Nature*, 2008, **451**, 315–317.
- 40 A. Yahia, P. L. Arnold, J. B. Love and L. Maron, *Chem. Commun.*, 2009, 2402–2404.
- 41 A. Yahia, P. L. Arnold, J. B. Love and L. Maron, *Chem.-Eur. J.*, 2010, **16**, 4881–4888.
- 42 M. W. Löble, J. M. Keith, A. B. Altman, S. C. E. Stieber, E. R. Batista, K. S. Boland, S. D. Conradson, D. L. Clark, J. Lezama Pacheco, S. A. Kozimor, R. L. Martin, S. G. Minasian, A. C. Olson, B. L. Scott, D. K. Shuh, T. Tylliszczak, M. P. Wilkerson and R. A. Zehnder, *J. Am. Chem. Soc.*, 2015, **137**, 2506–2523.

